Efficient water-soluble drag reducing star polymers with improved mechanical stability

David P. Cole[1], Ezat Khosravi [1], Osama M. Musa[2]

[1] Department of Chemistry, Durham University, Durham, DH1 3LE, United Kingdom

[2] Ashland Specialty Ingredients, Bridgewater, New Jersey, 08807, United States

Correspondence to: E. Khosravi (E-mail: ezat.khosravi@durham.ac.uk)

ABSTRACT

We describe here the first example of the synthesis of 4-arm star poly(acrylic acid) for use as a water-soluble drag reducing agent, by applying Cu(0)-mediated polymerization technique. High molecular weight 4-arm star poly(*tert*-butyl acrylate) (M_n = 3.0-9.0 x 10^5 g mol^{-1}) was first synthesized using 4,4'-oxybis(3,3-bis(2-bromopropionate)butane as an initiator and a simple Cu(0)/TREN catalyst system. Then, 4-arm star poly(*tert*-butyl acrylate) were subjected to hydrolysis using trifluoroacetic acid resulting in water-soluble 4-arm star poly(acrylic acid). Drag reduction test rig analysis showed 4-arm star poly(acrylic acid) to be effective as a drag reducing agent with drag reduction of 24.3 %. Moreover, 4-arm star poly(acrylic acid) exhibited superior mechanical stability when compared with a linear poly(acrylic acid) and commercially available drag reducing polymers; Praestol and poly(ethylene oxide). The linear poly(acrylic acid), Praestol and poly(ethylene oxide) all showed a large decrease in drag reduction of 8-12 % when cycled 30 times through the drag reduction test rig whilst, in contrast, 4-arm star poly(acrylic acid) demonstrated much higher mechanical stability.

INTRODUCTION

Fluids experience a friction or drag when travelling through pipes, resulting in a pressure drop. In 1948, Toms observed a reduction in friction after the addition of a small quantity of high molecular weight (HMW) polymer to turbulent pipe flow.[1] The 'drag reducing polymers' have many potential applications as they increase flow rate for liquids with the same energy cost. Water-soluble drag reducing polymers have oil field applications, e.g., fracking, acid stimulation and secondary oil recovery.[2] They also have many non-oil field applications for example field irrigation and slurry transport.[3, 4] Despite an incomplete understanding of the mechanism of drag reduction (DR), successful systems have been developed based around the requirement for ultra-high molecular weight (UHMW) polymers. Whilst natural polymers such as guar gum, xanthan gum, hydroxyethyl cellulose (HEC) and carboxymethyl cellulose (CMC) are all effective drag reducing agents (DRAs), their susceptibility to biodegradation is a problem.[5,6] Therefore, synthetic polymers are favored commercially due to their resistance to biodegradation. Poly(ethylene oxide) (PEO) is a synthetic polymer which can provide good drag reducing effects,[7] however, it is highly susceptible to mechanical degradation in shear flow.[8] Polyacrylamide (PAM) and its partially hydrolyzed analogues are most commonly used in commercial aqueous DR applications.[2,9] The presence of side groups in PAM has been shown to increase mechanical stability and it has been synthesized to UHMW using inverse-emulsion free radical polymerization.[10] However, the use of acrylamide is highly restricted by recent REACH (Registration, Evaluation, Authorisation and Restriction of Chemicals, 2006) regulations due to its carcinogenicity. Furthermore, the use of polymer emulsions without purification releases significant quantities of oil and surfactant, damaging the environment.

Decreasing the degradation of polymer DRAs remains a very important issue. The correlation between mechanical degradation of polymer chains and molecular weight is well established.[11] The mid-point chain scission theory dictates that, upon mechanical degradation, breakage occurs at the centre of a polymer chain, quickly reducing the polymer molecular weight/size.[8] In turbulent flow, polymers experience very high strain rates and breakage can occur within seconds of injection to the pipe, rendering the DRA ineffective. Resistance to mechanical degradation is, therefore, considered as important as drag reducing efficiency (DRE) when testing the suitability of polymer solutions.[12] As early as 1974, Little *et al.* observed that branched polymers are effective DRAs and are more stable to mechanical degradation.[8,13,14] It has been reported that, in contrast to HMW linear polymers, star polymers show higher resistance to mid-point chain scission, leading to a smaller decrease in molecular weight. It has also been suggested that less branched star polymers with HMW arms are likely to be the most effective systems for DRE and mechanical stability.[8,15]

Cu(0)-catalyzed polymerizations have been widely studied, allowing controlled polymerization in a range of systems.[16,17] The ease of catalyst handling, recovery and recycling from reaction mixture provides several benefits over conventional Atom Transfer Radical Polymerization (ATRP) methods.[18,19] There has been huge debate over the mechanism of these zero valent metal catalyzed polymerizations within the literature.[20-36] The first mechanism could be viewed as an extension of activator regenerated by electron transfer (ARGET) ATRP, proceeding *via* inner sphere electron transfer (ISET) and dominated by a fast alkyl halide activation step by Cu(I). Deactivation occurs due to Cu(II) which accumulates in the system as a result of a process similar to the persistent radical effect (PRE). Cu(0) acts as a supplemental activator, and reduces Cu(II) to regenerate Cu(I) in a method known as supplemental activator and reducing agent (SARA) ATRP.[37] The second mechanism, single electron transfer-living radical polymerization (SET-LRP), was proposed by Percec and is characterized by heterogeneous activation using Cu(0) in an outer sphere electron transfer (OSET) mechanism *via* a radical-anion intermediate.[38] Cu(II) deactivator is generated in the system by instantaneous and complete disproportionation of Cu(I).[38] Irrespective of which mechanism is correct, Cu(0) catalysis can be useful for the rapid synthesis of HMW polymers, including stars, at ambient temperatures in environmentally friendly aqueous solvent systems.[26,38,39] The resulting polymers are reported to contain low copper contamination (< 1 ppm).[26]

The work presented here describes the first example of the synthesis of 4-arm star poly(acrylic acid) (PAA) for application as an efficient water-soluble DRA. This is achieved *via* the Cu(0)-mediated polymerization of *tert*-butyl acrylate (*t*BA) using a 4-site initiator, followed by hydrolysis of P*t*BA to PAA using trifluoroacetic acid (TFA). A simple catalyst system, amenable to a commercial process, is used to produce 4-arm star polymers as efficient DRAs with enhanced mechanical stability.

EXPERIMENTAL SECTION

Materials

4,4'-Oxybis(3,3-bis(2-bromopropionate)butane (4AE) initiator was synthesized within the group by Dr Iain Johnson according to literature procedure.[40] Methyl 2-bromopropionate (MBP), dimethyl sulfoxide (DMSO, anhydrous ≥ 99.9 %), tris(2-aminoethyl)amine (TREN, 97 %) and trifluoroacetic acid (TFA, 99 %) were purchased from Sigma Aldrich and were used without further purification. Analytical grade methanol was purchased from Fisher Scientific and used as received. *tert*-Butyl acrylate (*t*BA, 99 %, stabilized with 15 ppm 4-methoxyphenol) was purchased from Alfa Aesar and used without further purification. Deuterated solvents for NMR analysis were purchased from Goss Scientific (D_2O) or Apollo Scientific ($CDCl_3$). Bare copper wire (24 standard wire gauge, diameter = 0.559 mm) was purchased from Fisher Scientific and used without further purification. Praestol (PAM) for drag reduction testing was provided by Ashland Inc. as an inverse-emulsion (0.5 wt%

polymer). Poly(ethylene oxide) ($M_v \approx 8 \times 10^6$ g mol^{-1}, PEO-8M) was purchased from Sigma Aldrich and used as received. Stock solutions of HMW polymer samples for drag reduction testing were prepared at a concentration of 0.5 wt% by stirring in distilled water for several days to provide a fully homogeneous solution. The solutions were further diluted to the required dose during testing.

Characterization

NMR spectra were recorded using a Bruker Avance-400 spectrometer operating at 400 MHz. $CDCl_3$ or D_2O were used as solvent and the spectra were referenced to the solvent trace (at 7.26 ppm - $CDCl_3$ and 4.79 ppm - D_2O). Molecular weight analysis of polymer molecules was obtained using size exclusion chromatography (SEC). Specifically a Viscotek TDA 302 using two 7.5 mm x 300 mm PLgel 5 μm mixed C columns and THF as the eluent (flow rate of 1 ml min^{-1}) at 35°C. Triple Detection SEC (refractive index (RI), viscosity and light scattering detectors) was used to determine molecular weights. These detectors were calibrated with narrow molecular weight distribution polystyrene as a standard, using a *dn*/*dc* (differential index of refraction) of 0.539 mL g^{-1} determined for 4-arm star P*t*BA.[41]

General procedure for the synthesis of linear and 4-arm star poly(*tert*-butyl acrylate)

Initiator (MBP or 4AE) and TREN were weighed into individual vials. DMSO was added to the TREN to prepare a stock solution. A portion of TREN solution (volume dependent on quantity of TREN required) was added to the initiator, followed by the addition of *t*BA and further DMSO, if necessary. The mixture was transferred to a Schlenk tube. Cu(0) wire was wrapped around a magnetic stirrer bar and was held above the reaction mixture using a magnet attached to the outside wall of the flask. The flask was sealed using a rubber septum and the mixture deoxygenated by bubbling with N_2. The flask was placed in an oil bath at

25 ^{o}C and the polymerization reaction was initiated by submerging the Cu(0)/stirrer. The mixture was stirred for the appropriate time and the polymerization was terminated by removing the Cu(0)/stirrer from the reaction mixture. THF was added to dissolve the resulting product and the conversion was determined using ^{1}H NMR spectroscopy in $CDCl_3$, by comparing the integration of the resonance due to a vinyl proton of monomer at 5.68 ppm with a resonance due to the *tert*-butyl of the polymer side chain at 1.42 ppm. The solution was then diluted with THF and was added to methanol:water (50:50, v:v) to precipitate the product which was isolated and dried in an oven under reduced pressure at 40°C. ^{1}H NMR (400 MHz, $CDCl_3$); 1.42 ppm ($-(CH_3)_3$); 1.5 - 1.8 ppm ($-CH_2$); 2.20 ($-CH$).

Measurement of Reaction Kinetics

In order to study the reaction kinetics on a small scale, parallel reactions (following the general procedure) using 4AE initiator were conducted for increasing reaction times. Reaction quantities used; *t*BA (0.71 g, 5.6 mmol), 4AE (18.6 mg, 0.024 mmol), TREN (1.4 mg, 0.009 mmol), DMSO (0.25 ml), Cu(0) wire (4.2 cm, 0.07 g).

Large Scale Polymerizations

The general procedure was followed for the large scale polymerization of *t*BA with reaction times between 24-72 h, using the following quantities; Star-P*t*BA1: $[M]_0:[I]_0 = 2360$, *t*BA (35.50 g, 278 mmol), 4AE (94.0 mg, 0.118 mmol), TREN (17.3 mg, 0.118 mmol), DMSO (12.50 ml), Cu(0) wire (210 cm, 3.58 g); Star-P*t*BA2: $[M]_0:[I]_0 = 7804$, *t*BA (10.00 g, 78.0 mmol), 4AE (7.9 mg, 0.010 mmol), TREN (1.5 mg, 0.010 mmol), DMSO (3.50 ml), Cu(0) wire (59 cm, 1.00 g); and Linear-P*t*BA: $[M]_0:[I]_0 = 2360$, *t*BA (35.50 g, 278 mmol), MBP (18.9 mg, 0.118 mmol), TREN (17.3 mg, 0.118 mmol), DMSO (12.50 ml), Cu(0) wire (210 cm, 3.58 g).

Hydrolysis of poly(*tert*-butyl acrylate) to poly(acrylic acid)

P*t*BA (0.25 g, 5.0 μmol, 2.0 mmol *tert*-butyl groups), was transferred to a round bottomed flask fitted with a magnetic stirrer bar and water condenser. DCM (9 ml) was added to the flask and the mixture stirred for 3 h until it became homogeneous. TFA (0.77 ml, 1.14 g, 10.0 mmol) was injected in to the flask and stirred at room temperature for 40 h. The reaction mixture became heterogeneous and the solid polymer was isolated by the removal of DCM/TFA solution. The PAA product was dried under a flow of nitrogen to remove DCM and excess TFA and analysed by ^{1}H NMR spectroscopy in D_2O. ^{1}H NMR (400 MHz, D_2O); 1.25-1.75 ($-CH_2$); 2.10 ($-CH$).

Testing of Drag Reduction

Testing of drag reduction efficiency was conducted using tap water. The water typically had a pH of 7.61, and a Ca, Mg and Na content of 27.63 mg dm^{-3}, 11.84 mg dm^{-3} and 7.56 mg dm^{-3}, respectively. In order to measure the DRE of synthesized polymers a drag reduction test rig (Supporting Information, Figure S2 and S3) was used. The rig allowed the calculation of percentage drag reduction (*%DR*) by measuring the time taken for a known volume of dilute polymer solution to travel a known distance through a pipe, followed by comparison with a pure water sample. If drag reduction occurs, flow rate increases relative to pure water control. The full discussion of the testing procedure and calculation of *%DR* is provided in Supporting Information (Figure S2-S5, Table S1-S7, Equation S1-S4).

Testing of Mechanical Stability

To study the resistance of a polymer sample to mechanical degradation, the *%DR* was first measured for the sample as described in the Supporting Information. The polymer solution was then cycled through the drag reduction test rig for 30 runs (pressure = 30 Psi) and the flow rate was recorded for each run. The *%DR* was then measured again for the resulting solution.

RESULTS AND DISCUSSION

Synthesis of 4-arm star and linear poly(*tert*-butyl acrylate)

Acrylic acid cannot be directly polymerized using Cu-mediated polymerization techniques due to interactions with the copper catalyst, therefore, *tert*-butyl acrylate (*t*BA) is commonly used as a protected monomer in the synthesis of PAA.[42-46] In this work, 4,4'-oxybis(3,3-bis(2-bromopropionate)butane (4AE) is used as an initiator in the polymerization of *t*BA applying a Cu(0)/TREN catalyst system to synthesize 4-arm star P*t*BA (Scheme 1). Several measures are often used in Cu(0)-mediated polymerizations to gain high levels of control, such as; cleaning of copper wire, addition of $CuBr_2$ and Me_6-TREN ligand. It should be noted that these measures increase cost and environmental impact of a commercial process. Hence, a simple and economically viable catalyst system is used, based on Cu wire and TREN ligand which is 10 x cheaper than Me_6-TREN.[47] Importantly, TREN has been shown to provide a similar level of control when directly compared with Me_6-TREN.[48] Previously, the 4AE initiator has been used by Trzebicka *et al.* in the synthesis of HMW star shaped P*t*BA *via* conventional ATRP techniques (CuBr/PMDETA/acetone). However, in this system monomer conversion was restricted to 40 % in order to prevent star-star coupling.[41,49] The reactions described here are conducted in DMSO, a very effective solvent for Cu(0)-mediated polymerizations.[26] Furthermore, due to the insolubility of P*t*BA in DMSO above $M_n \approx 2000$ g mol^{-1}, a biphasic reaction mixture is generated during the polymerization which has been shown to decrease the copper contamination in the final product and reduce bimolecular termination at high conversion in the synthesis of branched molecules.[50,51] Despite the formation of a biphasic system, control has been reported for the polymerization of butyl acrylate (*n*BA) and *t*BA using ethylene bromoisobutyrate initiator.[50,51]

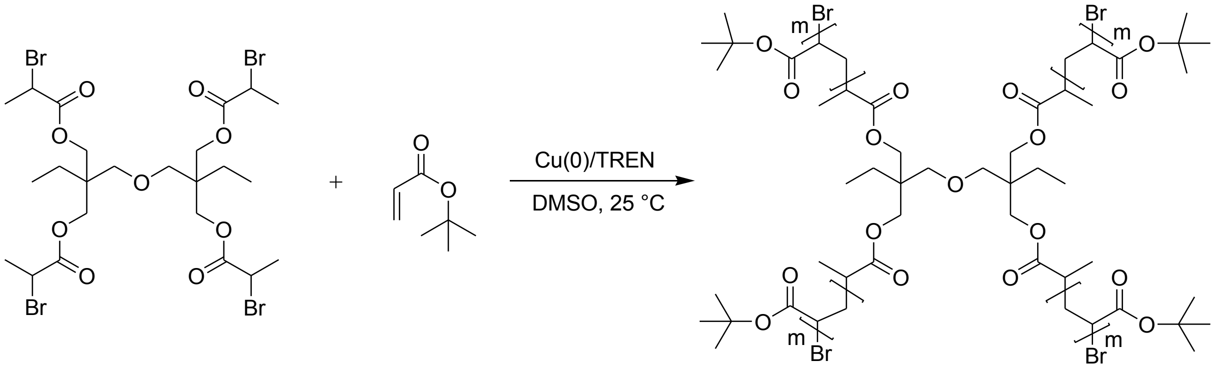

4AE **tBA** **Star-PtBA**

Scheme 1: Polymerization of *t*BA using 4,4'-oxybis(3,3-bis(2-bromopropionate)butane, 4AE, initiator.

The ratio of $[t\text{BA}]_0:[4\text{AE}]_0:[\text{TREN}]_0$ of 236:1:0.4, targeting a molecular weight of $\approx 3.1 \times 10^4$ g mol^{-1}, was used to investigate the kinetics of the polymerization by conducting parallel reactions on a small scale.

A linear increase of conversion with time is observed in the early stages of the reaction (< 500 min), Figure 1a, (■), reaching 75 % after 8 h. At longer reaction times, the graph levels off and the reaction does not progress beyond 80 % conversion, believed to be due to the high viscosity of the mixture. The reaction mixture became biphasic at low conversion due to the insolubility of P*t*BA in DMSO. The two phases first formed a stable emulsion with small polymer droplets dispersed in the DMSO/monomer solution. However, as the reaction progressed, monomer was converted to polymer and the volume of the DMSO/monomer layer decreased. The upper polymer layer then agglomerated, becoming extremely viscous and as a result the polymerization became diffusion limited. This may be responsible for the limit of 80 % for the conversion of monomer to polymer.

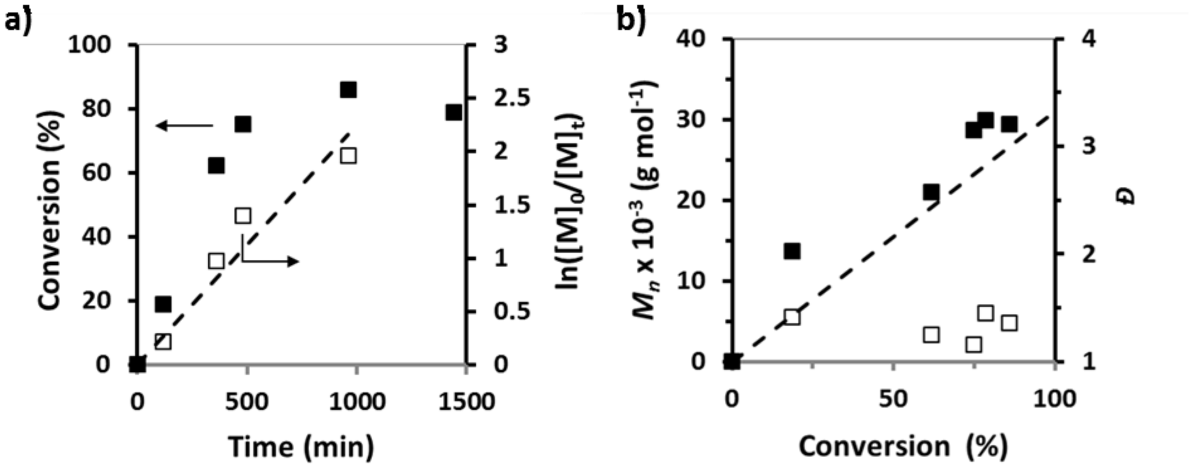

Figure 1: Polymerization of *t*BA using 4AE, $[M]_0$:$[I]_0$:$[L]_0$ =236:1:0.4; **a)** Conversion (■) and $\ln([M]_0/[M]_t)$ (□) vs time; **b)** M_n(SEC) (■) and *Đ* (□) vs conversion. (M_n(Theor) shown by dashed line).

The kinetic plot of $\ln([M]_0/[M]_t)$ vs time in Figure 1a (□) also shows a linear increase for the first 960 min of the reaction suggesting a constant concentration of radicals in the solution. An apparent rate constant of propagation of k_p^{app} = 0.0022 min^{-1} was calculated, which is comparable to the values reported by Percec for the polymerization of *n*BA in a homogeneous mixture of DMSO and tetrafluoropropanol (TFP) (k_p^{app} = 0.0014-0.0061 min^{-1}).[52] The k_p^{app} of our system is low in comparison to the polymerization of MA in DMSO (k_p^{app} = 0.044 min^{-1}), using an equivalent catalyst surface area.[53] This is possibly due to the increased steric bulk of the *t*BA monomer. The graphs in Figure 1b relate monomer conversion with M_n(SEC) (■) and *Đ* (□). The theoretical molecular weight M_n(Theor) at each conversion was calculated using Equation 1 and is indicated in the figure by the dashed black line.

$$M_n(\text{Theor}) = \text{MW}_{t\text{BA}} \times \left(\frac{[t\text{BA}]_0}{[\text{I}]_0} \times \frac{\%\text{Conv}}{100} \right) + \text{MW}_\text{I} \qquad \textbf{(Equation 1)}$$

At low conversion, M_n(SEC) (13.7 x 10^3 g mol^{-1}) is significantly higher than the theoretically calculated value (6.4 x 10^3 g mol^{-1}). This indicates a higher rate of propagation than initiation, and may be a consequence of rate acceleration due to the formation of a biphasic system in the early stages of the reaction. As the polymerization progresses, $CuBr_2$ deactivator is formed in more significant quantities and the reaction becomes more controlled. This can be observed by the linear increase of M_n(SEC) at higher conversion and the closer correlation with M_n(Theor). Throughout the reaction the polymer molecular weight dispersity remained between $Đ = 1.15 – 1.45$ (Figure 1b). This compares favorably to the polymerization of *t*BA ($M_n = 3 \times 10^3$ g mol^{-1}, $Đ = 1.47$) described in the literature in DMSO, using Cu(0)/$CuBr_2$/Me_6-TREN and ethyl bromoisobutyrate initiator.[50]

The SEC chromatograms for the reactions display a shift towards lower retention volume and, therefore, higher molecular weight with time (Figure 2). At higher conversion, a near symmetrical peak is observed, suggesting the absence of undesirable star-star coupling. Similar results were reported by Haddleton *et al.* for the synthesis of an 8-arm P*n*BA star in DMSO to high conversion.[51]

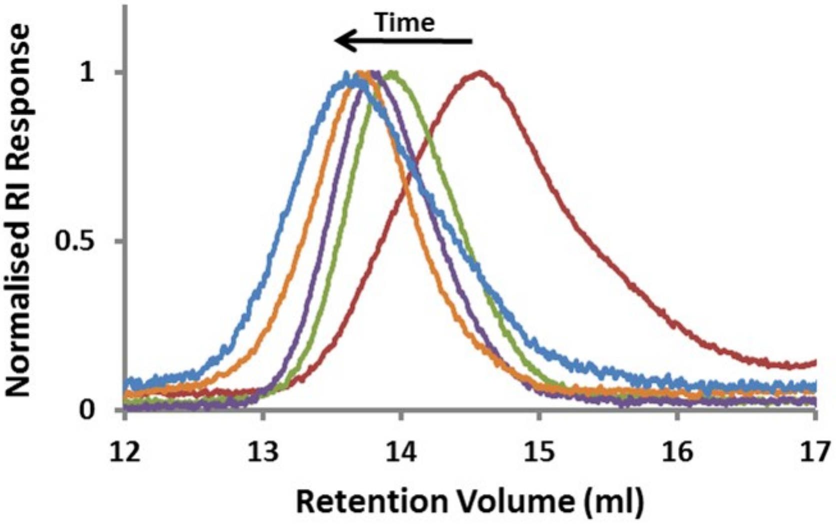

Figure 2: Plot of RI vs retention volume demonstrating shift to higher molecular weight with time for the polymerization of *t*BA using 4AE, $[M]_0:[I]_0 = 236$. Red line = 120 min; green line = 360 min; purple line = 480 min; orange line = 960 min; blue line = 1440 min.

The ^{1}H NMR spectrum of Star-P*t*BA product (Figure 3) shows distinctive broad resonances at 1.8 ppm (**a**) and 2.2 ppm (**b**) and at 1.4 ppm (**e**), characteristic of the backbone and side chain of P*t*BA, respectively. The resonances corresponding to the core molecule can also be clearly seen at 0.8 ppm (**4**), 3.3 ppm (**1**) and 3.8-4.2 ppm (**5**).

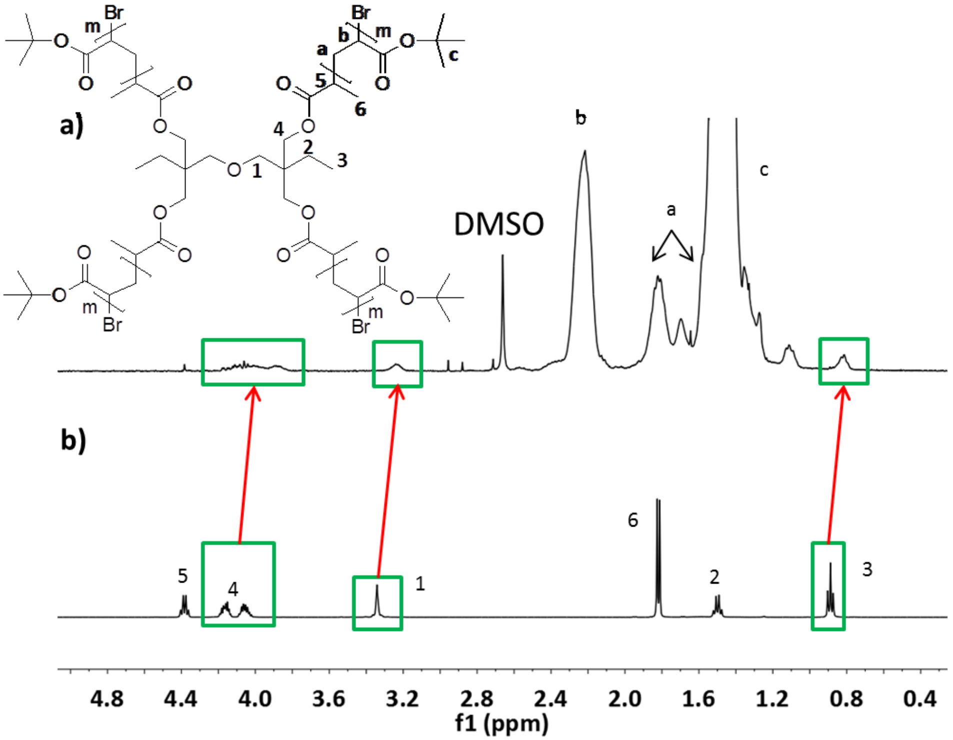

Figure 3: 400 MHz-^{1}H NMR spectrum of; a) P*t*BA initiated using 4AE; b) 4AE initiator.

The molecular weight for each star P*t*BA sample was also calculated from the ^{1}H NMR spectrum by comparing the integration of the core resonance due to **1** (4H), with the resonance of **b** for the polymer backbone (1H) using Equation 2.

$$M_n(\mathrm{NMR}) = \left(\frac{\int \mathbf{b} \times 4}{\int \mathbf{1}} \times\ 128.17\ \mathrm{g\ mol^{-1}} \right) +\ 790.17\ \mathrm{g\ mol^{-1}} \quad \textbf{(Equation 2)}$$

Where 128.17 g mol^{-1} is the mass of monomer repeat unit and 790.17 g mol^{-1} is the mass of the 4AE core, assuming retention of Br at the polymer chain ends. The molecular weight values estimated (□) are shown to be in good agreement with M_n(Theor) (dashed line) and M_n(SEC) (■), Figure 4. The results indicate that the simple Cu(0)/TREN catalyst system is effective in the controlled synthesis of star P*t*BA in DMSO with a target molecular weight of 3 x 10^4 g mol^{-1}.

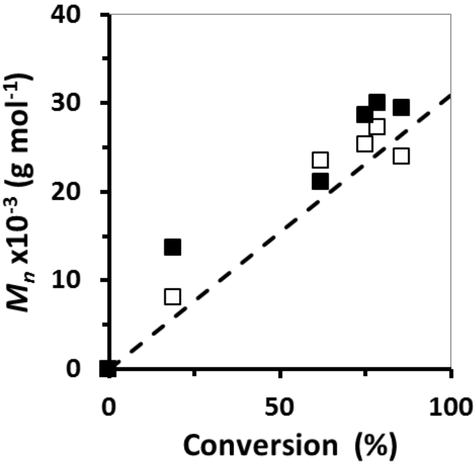

Figure 4: Plot of M_n(NMR) (□) vs monomer conversion. M_n(Theor) (dashed line) and M_n(SEC) (■) are included for comparison.

A ratio of [*t*BA]$_0$:[4AE]$_0$:[TREN]$_0$ of 2360:1:1 was used to synthesize star P*t*BA with a molecular weight of 3 x 10^5 g mol^{-1} (Star-P*t*BA1, Table 1, Entry vi). The M_n(SEC) (3.09 x 10^5 g mol^{-1}) was significantly higher than M_n(Theor) (2.08 x 10^5 g mol^{-1}), however, the narrow dispersity ($Đ$ = 1.30) suggested control was maintained over the polymerization. Moreover, the ratio of [*t*BA]$_0$:[4AE]$_0$:[TREN]$_0$ = 7804:1:1 was used to synthesize Star-P*t*BA2 with a target molecular weight of 1 x 10^6 g mol^{-1} (Table 1, Entry vii). The M_n(SEC) (8.61 x 10^5 g mol^{-1}) closely matched M_n(Theor) (8.50 x 10^5 g mol^{-1}) with a dispersity of $Đ$ = 1.61. In order to compare the drag reducing properties of star polymers with a linear analogue, a polymerization reaction of *t*BA was also conducted using methyl 2-bromopropionate (MBP) as an initiator. A [*t*BA]$_0$:[MBP]$_0$:[TREN]$_0$ of 2360:1:1 was used to target linear P*t*BA with a molecular weight of 3 x 10^5 g mol^{-1} (Linear-P*t*BA, Table 1, Entry viii). The linear polymer exhibited a M_n(SEC) of 7.69 x 10^5 g mol^{-1} which was much higher than the theoretical value (2.73 x 10^5 g mol^{-1}), with a broad molecular weight distribution ($Đ$ = 2.29), demonstrating poor control over the polymerization. This is believed to be due to the decreased steric hindrance of the MBP initiator compared to 4AE which allows more rapid agglomeration of the polymer layer in the biphasic system, preventing access of $CuBr_2$ to the active chain ends.

However, the difference in $Đ$ could also be due to the MWD averaging effect in 4 arms of the star polymer. The intrinsic viscosities obtained using SEC analysis show a much lower value for the Star-P*t*BA2 sample (2.16 dL g^{-1}), in comparison to that of Linear-P*t*BA (3.70 dL g^{-1}), despite having similar molecular weights. This is expected due to the more compact structure of the star macromolecule.

The conversion vs polymerization time was not optimized for the syntheses of Star-PtBA1 (entry vi) and Star-PtBA2 (entry vii) as the reactions were carried out on 35.5g and 10g scale, respectively, as indicated at the bottom of Table 1. The reaction mixture in the case of Star-PtBA1 became very viscous due to the scale and it could not be regularly sampled to follow the reaction conversion with time. Therefore, the reaction was stopped after 70 h to ensure high conversion.

Table 1: Polymerization results from kinetic study (**i**-**v**) and large scale polymerizations (**vi**-**viii**) of *t*BA in DMSO using 4AE and MBP initiators**.**

Entry	Sample Code	M_n(Target) x 10^{-5} (g mol^{-1})	Time (h)	Conv. (%)	M_n(Theor) x 10^{-5} (g mol^{-1})	M_n(SEC) x 10^{-5} (g mol^{-1})	*Đ*	*IV* (dL g^{-1})
i	Star-P*t*BA-kin	0.3	2	19	0.06	0.13	1.41	-
ii	Star-P*t*BA-kin	0.3	6	62	0.19	0.23	1.25	-
iii	Star-P*t*BA-kin	0.3	8	75	0.23	0.31	1.15	-
iv	Star-P*t*BA-kin	0.3	16	86	0.27	0.29	1.36	-
v	Star-P*t*BA-kin	0.3	24	79	0.24	0.35	1.45	-
vi	Star-P*t*BA1	3.0	70	69	2.08	3.09	1.30	0.76
vii	Star-P*t*BA2	10.0	24	85	8.50	8.61	1.61	2.16
viii	Linear-P*t*BA	3.0	44	91	2.73	7.69	2.29	3.70

NB: Quantity of Monomer **vi/viii** = 35.5 g, **vii** = 10 g.

Synthesis of high molecular weight 4-arm star and linear poly(acrylic acid) for DR testing

Star-P*t*BA1, Star-P*t*BA2 and Linear-P*t*BA were subjected to hydrolysis using TFA to prepare water-soluble PAA (Star-PAA1, Star-PAA2 and Linear-PAA) for DR testing (Scheme 2). TFA is particularly useful due to the ability to selectively cleave *tert*-butyl (*t*Bu) groups whilst leaving other esters within the same polymer intact.[54]

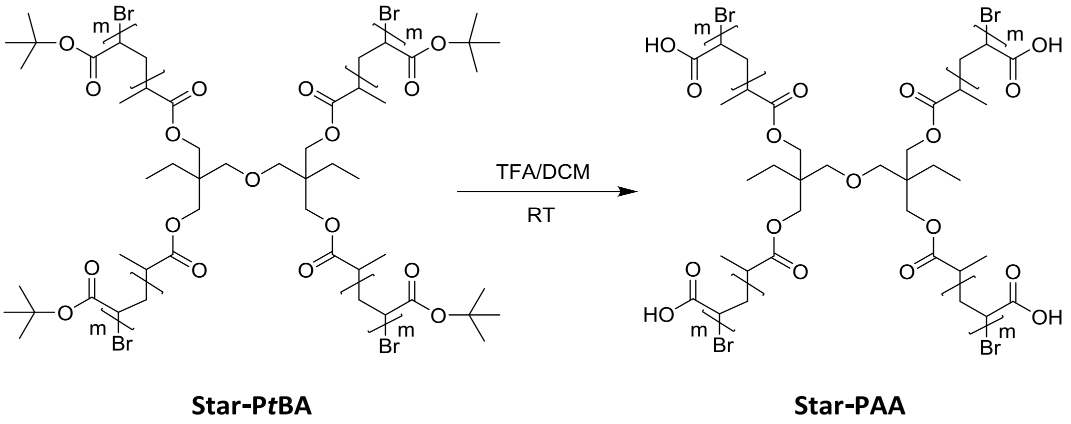

Scheme 2: Hydrolysis of PtBA to PAA using TFA/DCM.

The hydrolysis reaction was first conducted in an NMR tube using $CDCl_3$ to monitor the reaction progress by following the decrease in intensity of the resonance due to the *t*Bu side chains at 1.42 ppm (Figure 5i, e). Moreover, the increase in the intensity of the resonance corresponding to *tert*-butyl trifluoroacetate side-product at 1.58 ppm (Figure 5ii-v, E), can be observed as the reaction progresses. The comparison of the two resonances (e and E) allows calculation of the ratio of *tert*-butyl trifluoroacetate to *tert*-butyl side chains and indicates that complete hydrolysis is achieved after 24 h.

The hydrolysis reactions on a larger scale were left for 40 h. Comparison of the ^1H NMR spectrum before and after the reaction demonstrated complete hydrolysis giving a fully water-soluble PAA sample (Supporting Information, Figure S1).

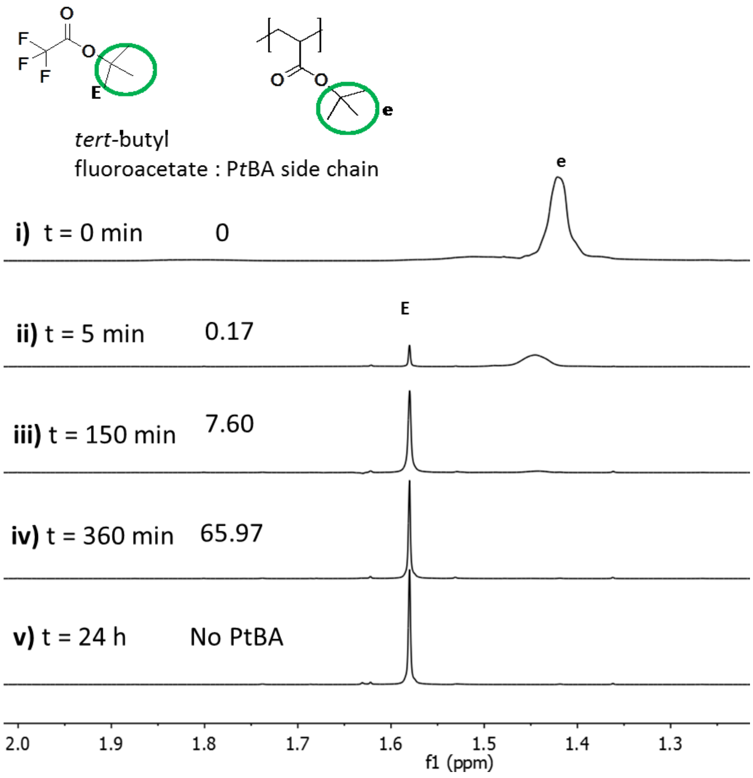

Figure 5: 400 MHz-^{1}H NMR spectra showing hydrolysis of Star-P*t*BA2 at increasing time from **i** - **v**.

Testing of drag reducing properties of 4-arm star and linear poly(acrylic acid)

The star and linear PAA samples were tested for their DRE and the results are summarized in Table 2. Star-PAA1 and Star-PAA2 (Table 2, Entry i-ii) with a lower and higher molecular weight, respectively, provided a direct comparison of *%DR* dependence. The graphs of *%DR* vs dose for Star-PAA1 and Star-PAA2 are plotted in Figure 6a. It is clear that the lower molecular weight Star-PAA1 is ineffective as a DRA; *%DR* does not reach above 5 %, even at high dose. In contrast, for the higher molecular weight Star-PAA2, *%DR* rises with dose to a maximum ($\%DR_{MAX}$, defined as maximum value measured in test) of 24 % at a dose of 190 ppm. A maximum value is reached as the drag reducing effect of the applied HMW polymer is counter-balanced by an increased solution viscosity. The plot for *%DR* vs dose for Linear-PAA (Table 2, Entry iii), Figure 6a, also shows a similar $\%DR_{MAX}$ (24 % at 100 ppm). The correlation between $\%DR_{MAX}$ values for Linear-PAA and Star-PAA2 of similar molecular weight suggests that the polymer topology does not have a significant impact on the DRE of the system. If the linear polymer was much more effective as a DRA, a significantly higher *%DR* compared to the star polymer would be expected at equivalent molecular weight.

Table 2: Summary of molecular weight and DRE data for polymer samples tested using drag reducing rig.

Entry	Sample Code	Polymer Type	M_n x 10^{-5} (g mol^{-1})	*DP* x 10^{-3}	*Đ*	$\%DR_{MAX}$	Dose (ppm)	*%DR* at 190 ppm
i	Star-PAA1	PAA	1.77^+	2.41	1.30	3	330	1
ii	Star-PAA2	PAA	4.84^+	6.71	1.61	24	190	24
iii	Linear-PAA	PAA	4.32^+	6.00	2.29	24	100	22
iv	Praestol	PAM	~200*		N/A	37	5.0	N/A
v	PEO-8M	PEO	80*		N/A	57	10.0	N/A

+ = M_n values measured for P*t*BA samples using THF SEC and adjusted assuming full hydrolysis of P*t*BA to PAA; * = M_w based on suppliers intrinsic viscosity measurements.

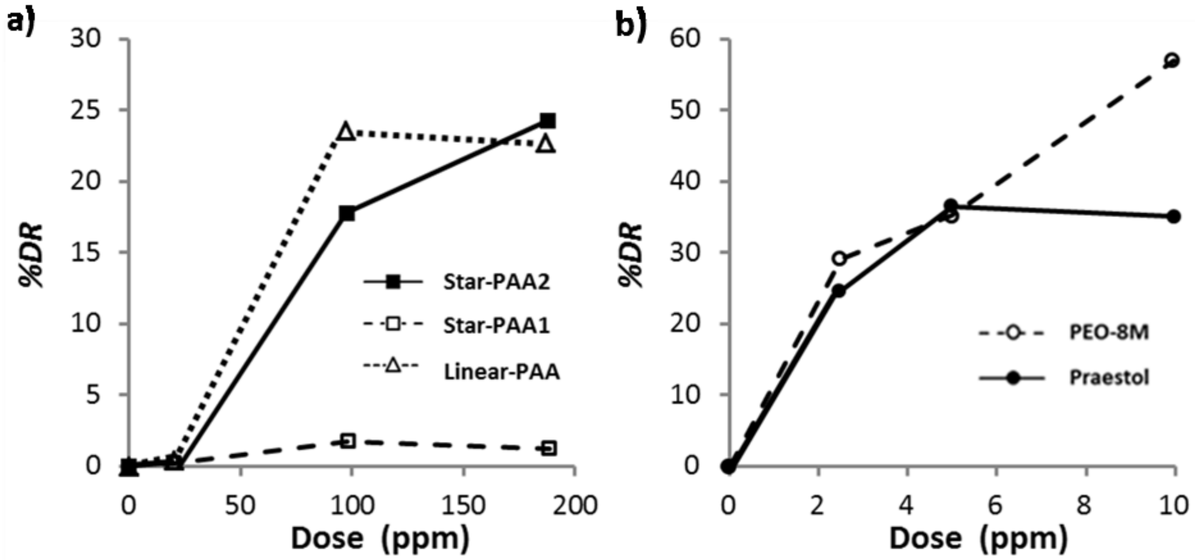

Figure 6: Plot of *%DR* vs Dose (ppm); **a)** Star and linear PAA synthesized using Cu(0)-mediated polymerization; **b)** Commercial polymer samples.

Two commercial polymers, Praestol and PEO-8M, with known drag reducing properties were investigated to evaluate the suitability of the test rig and to provide basis for comparison with the PAA samples synthesized here. The graph of *%DR* with dose for the Praestol sample (Table 2, Entry iv) is shown in Figure 6b, demonstrating a sharp increase in *%DR* with dose up to 5 ppm ($\%DR_{MAX}$ = 37 %). Measurements carried out on PEO-8M (Table 2, Entry v), demonstrated $\%DR_{MAX}$ of 57 % at 10 ppm (Figure 6b). The commercial polymers are shown to be more effective at a lower dose when compared to Star-PAA2 and Linear-PAA. In the case of Praestol, this is due to the UHMW (≈ 15-20 x 10^6 g mol^{-1}) which can only be synthesized using a free-radical inverse emulsion polymerization technique. In the case of PEO, although the molecular weight (8 x 10^6 g mol^{-1}) is lower than Praestol, the $\%DR_{MAX}$ is higher, most likely due the high flexibility of the polymer backbone chain.

Testing of mechanical stability of 4-arm star and linear poly(acrylic acid)

Star-PAA2 and Linear-PAA, with high DRE, were tested for their mechanical stability by following the change in flow rate and *%DR* over 30 runs through the test rig and the data is summarized in Table 3.

Table 3: Summary of drag reduction and mechanical stability (after 30 runs through test rig) data for polymer samples tested using drag reducing rig.

Entry	Sample Code	$\%DR_{MAX}$	Dose (ppm)	*%DR* at 190 ppm	% Change of flow rate	Ave. Change in *%DR*
i	Star-PAA2	24	190	24	-0.5	+3
ii	Linear-PAA	24	100	22	-12.8	-10
iii	Praestol	37	5.0	N/A	-10.2	-12
iv	PEO-8M	57	10.0	N/A	-8.2	-9

Star-PAA2 (Table 3, Entry i) and Linear-PAA (Table 3, Entry ii) were tested at a dose of 190 ppm. The change in flow rate for Star-PAA2 is plotted in Figure 7 (raw data shown in Supporting Information, Figure S6). A small decrease (< 2 %) in flow rate is observed over 30 runs with a rate of decrease of just -0.03 ml s^{-1} run^{-1}. The results are interesting as they suggest negligible mechanical degradation of the polymer chain has occurred during the test.

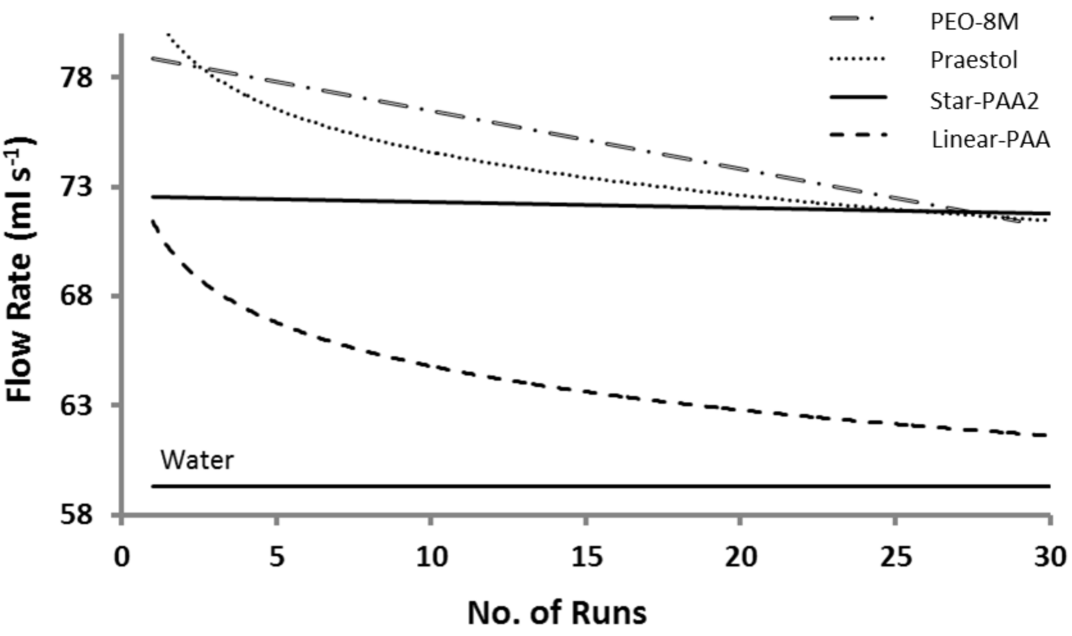

Figure 6: Change in flow rate for polymer solutions as they are repeatedly cycled through test rig for 30 runs.

The change in flow rate for Linear-PAA (Table 3, Entry ii) is also plotted in Figure 7 (raw data shown in Supporting Information, Figure S7). A much higher, exponential, decrease in flow rate is observed. The initial rate decrease of -2.9 ml s^{-1} run^{-1} for Linear-PAA is 10 times faster than for Star-PAA2 despite a similar molecular weight for these samples. The exponential decrease is expected if the chains are each broken at their centre as dictated by the mid-point chain scission theory. An overall decrease in flow rate of -13 % was observed for Linear-PAA between the first and thirtieth run with the final flow rate close to that of pure water. The comparison between linear and star polymers is considered to be evidence that the mechanical stability of PAA is improved as a result of the presence branching in its structure. The higher strength of a star polymer is thought to be a result of the distribution of forces through multiple polymer arms. In addition, the slower decrease in DRE observed in a star polymer may result from the individual cleavage of polymer arms. This greatly reduces the impact of polymer chain scission upon the overall molecular weight and hence DRE.

The commercial polymers; Praestol and PEO-8M (Table 3 Entry iii-iv) were then tested for their mechanical stability (Figure 7, raw data shown in Supporting Information, Figure S8 and S9). Measurements were conducted at the dose corresponding to $\%DR_{MAX}$; 5 ppm and 10 ppm for Praestol and PEO-8M, respectively. A fast decrease in flow rate with a total decrease of -10.2 % and -8.2 % over 30 runs was observed for Praestol and PEO-8M, respectively. Whilst the commercial polymers demonstrated $\%DR_{MAX}$ at a much lower dose than those synthesized here, the flow rate of Star-PAA2 (72 ml s^{-1}) is higher than for Praestol (71 ml s^{-1}) and equal to PEO-8M (72 ml s^{-1}) after 30 runs the through the test rig. This could be important for commercial applications where degradation of the polymer necessitates further doses to be added to maintain the drag reducing effect.

The Linear-PAA and commercial polymers ,Praestol and PEO-8M, demonstrate a large decrease for each polymer between 8-12 %. In contrast, the Star-PAA2 demonstrates a small increase in *%DR* of +3 %. The test for mechanical stability is a time consuming process and, therefore, the 30 run measurements were not repeated in order to establish the experimental error. Therefore, the +3 % increase may well be within the error of the measurement.

CONCLUSION

A simple catalyst system comprising Cu(0)/TREN and a 4-site initiator (4AE) was successfully used to synthesize 4-arm star P*t*BA, Star-PtBA1 and Star-PtBA2,with M_n of 3.09 x10^5 and 8.61 x 10^5 g mol^{-1}, respectively. In addition a linear analogue (Linear-PtBA) with a molecular weight of 7.69 x 10^5 g mol^{-1} was also synthesized. These HMW polymers were then hydrolyzed using TFA to prepare three water-soluble samples; Star-PAA1, Star-PAA2 and Linear-PAA for DR testing.

The DRE of the PAA samples was determined using a drag reduction test rig and compared with current commercial products (Praestol and PEO-8M). Whilst the lower molecular weight Star-PAA1 was ineffective as a DRA, the higher molecular weight Star-PAA2 demonstrated a significant $\%DR_{MAX}$ (24 %), comparable to Praestol (37 %). The Linear-PAA sample provided a $\%DR_{MAX}$ of 24 % suggesting the polymer topology does not have a significant impact on the DRE.

The mechanical stability of Star-PAA2 and Linear-PAA was compared with that of Praestol and PEO-8M. Whilst the degradation of Praestol and PEO-8M was significant, almost no change in flow rate was observed for Star-PAA2. This could be important for commercial applications where degradation of the polymer necessitates further doses to be added to maintain the drag reducing effect.

ACKNOWLEDGEMENT

We gratefully acknowledge Ashland Inc. for the financial support of this research.

REFERENCES

1 B. A. Toms, *J. Colloid Sci.* **1949**, 4, 511-521.

2 M. A. Kelland, *Production Chemicals for the Oil and Gas Industry*. CRC Press: 2009; Vol. 1, p 437.

3 M. V. Kameneva, Z. J. J Wu, A. Uraysh, B. Repko, K. N. Litwak, T. R. Billiar, M. P. Fink, R. L. Simmons, B. P. Griffith, H. S. Borovetz, *Biorheology* **2004**, 41, 53-64.

4 W. Brostow, *Ind. Eng. Chem.* **2008**, 14, 409-416.

5 J. W. Hoyt, *Trends Biotechnol.* **1985**, 3, 17-21.

6 C. L. McCormick, R. D. Hester, S. E. Morgan, A. M. Safieddine, *Macromolecules* **1990,** 23, 2124-2131.

7 N. J. Kim, S. Kim, S. H. Lim, K. Chen, W. Chun, *Int. Commun. Heat Mass* **2009**, 36, 1014-1019.

8 H. J. Choi, C. A. Kim, J. I. Sohn, M. S. Jhon, *Polym. Degrad. Stabil.* **2000**, 69, 341-346.

9 S. E. Morgan, C. L. McCormick, *Prog. Polym. Sci.* **1990**, 15, 507-549.

10 S. Reekmans, J. Irene, P. Cornet, Polyacrylamide polymerisation. 1998.

11 W. Kauzmann, H. Eyring, *J. Am. Chem. Soc.* **1940**, 3113-3125.

12 O. K. Kim, R. C.Little, R. L. Patterson, R. Y. Ting, *Nature* **1974**, 250, 408-410.

13 S. R. Deshmukh, R. P. Singh, *J. Appl. Polym. Sci.* **1986**, 32, 6163-6176.

14 S. R. Deshmukh, P. N. Chaturvedi, R. P. Singh, *J. Appl. Polym. Sci.* **1985**, 30, 4013-4018.

15 L. Xue, U. S. Agarwal, P. J. Lemstra, *Macromolecules* **2005**, 38, 8825-8832.

16 K. Matyjaszewski, S. Coca, S. G. Gaynor, M. L. Wei, B. E. Woodworth, *Macromolecules* **1997**, 30, 7348-7350.

17 A. D. Asandei, V. Percec, *J. Polym. Sci., Part A: Polym. Chem.* **2001**, 39, 3392-3418.

18 N. Chan, M. F. Cunningham, R. A. Hutchinson, *Macromol. Rapid Commun.* **2011**, 32, 604-609.

19 J. A. Burns, C. Houben, A. Anastasaki, C. Waldron, A. A. Lapkin, D. M. Haddleton, *Polym. Chem.* **2013**, 4, 4809-4813.

20 D. Konkolewicz, Y. Wang, P. Krys, M. Zhong, A. A. Isse, A. Gennaro, K. Matyjaszewski, *Polym. Chem.* **2014**, 5, 4396-4417.

21 Y. Wang, M. Zhong, W. Zhu, C.-H. Peng, Y. Zhang, D. Konkolewicz, N. Bortolamei, A. A. Isse, A. Gennaro, K. Matyjaszewski, *Macromolecules* **2013**, 46, 3793-3802.

22 M. Zhong, Y. Wang, P. Krys, D. Konkolewicz, K. Matyjaszewski, *Macromolecules* **2013**, 46, 3816-3827.

23 C.-H. Peng, M. Zhong, Y. Wang, Y. Kwak, Y. Zhang, W. Zhu, M. Tonge, J. Buback, S. Park, P. Krys, D. Konkolewicz, A. Gennaro, K. Matyjaszewski, *Macromolecules* **2013**, 46, 3803-3815.

24 D. Konkolewicz, Y. Wang, M. Zhong, P. Krys, A. A. Isse, A. Gennaro, K. Matyjaszewski, *Macromolecules* **2013**, 46, 8749-8772.

25 D. Konkolewicz, P. Krys, J. R. Góis, P. V. Mendonça, M. Zhong, Y. Wang, A. Gennaro, A. A. Isse, M. Fantin, K. Matyjaszewski, *Macromolecules* **2014**, 47, 560-570.

26 B. M. Rosen, V. Percec, *Chem. Rev.* **2009**, 109, 5069-5119.

27 A. A. Isse, A. Gennaro, C. Y. Lin, J. L. Hodgson, M. L. Coote, T. Guliashvili, *J. Am. Chem. Soc.* **2011**, 133, 6254-6264.

28 N. H. Nguyen, V. Percec, *J. Polym. Sci., Part A: Polym. Chem.* **2011**, 49, 4227-4240.

29 N. Zhang, S. R. Samanta, B. M. Rosen, V. Percec, *Chem. Rev.* **2014**, 114, 5848-5958.

30 M. E. Levere, N. H. Nguyen, V. Percec, *Macromolecules* **2012**, 45,8267-8274.

31 M. E. Levere, N. H. Nguyen, X. Leng, V. Percec, *Polym. Chem.* **2013**, 4, 1635-1647.

32 G. Lligadas, V. Percec, *J. Polym. Sci., Part A: Polym. Chem.* **2008**, 46, 6880-6895.

33 G. Lligadas, B. M. Rosen, C. A. Bell, M. J. Monteiro, V. Percec, *Macromolecules* **2008**, 41, 8365-8371.

34 M. E. Levere, N. H. Nguyen, H.-J. Sun, V. Percec, *Polym.Chem.* **2013**, 4, 686-694.

35 S. Harrisson, P. Couvreur, J. Nicolas, *Macromolecules* **2012**, 45, 7388-7396.

36 S. Harrisson, J. Nicolas, *ACS Macro Letters* **2014**, 3, 643-647.

37 Y. Zhang, Y. Wang, C.-H. Peng, M. Zhong, W. Zhu, D. Konkolewicz, K. Matyjaszewski, *Macromolecules* **2012**, 45, 78-86.

38 V. Percec, T. Guliashvili, J. S. Ladislaw, A. Wistrand, A. Stjerndahl, M. J. Sienkowska, M. J. Monteiro, S. Sahoo, *J. Am. Chem. Soc.* **2006**, 128, 14156-14165.

39 N. H. Nguyen, J. Kulis, H. J. Sun, Z. F. Jia, B. Van Beusekom, M. E. Levere, D. A. Wilson, M. J. Monteiro, V. Percec, *Polym. Chem.* **2013**, 4, 144-155.

40 I. J. Johnson, E. Khosravi, O. M. Musa, R. E. Simnett, A. M. Eissa, *J. Polym. Sci., Part A: Polym. Chem.* **2015**, 53, 775-786.

41 B. Mendrek, B. Trzebicka, W. Walach, A. Dworak, *Eur. Polym. J.* **2010**, 46, 2341-2351.

42 M. Maier, C. Dollendorf, H. Ritter, J. E. Klee, *Macromol. Chem. Phys.* **2012**, 213, 2598-2605.

43 Z. Shen, Y. Chen, E. Barriau, H. Frey, *Macromol. Chem. Phys.* **2006**, 207, 57-64.

44 Y. L. Zhao, Y. M. Chen, C. F. Chen, F. Xi, *Polymer*, **2005**, 46, 5808-5819

45 R. Francis, B. Lepoittevin, D. Taton, Y. Gnanou, *Macromolecules* **2002**, 35, 9001-9008

46 S. J. Hou, E. L. Chaikof, D. Taton, Y. Gnanou, *Macromolecules* **2003**, 36, 3874-3881

47 TREN (Prod. No. 225630) and Me_6-TREN (Prod. No. 723142), www.sigmaaldrich.com

48 N. H. Nguyen, M. E. Levere, V. Percec, *J. Polym. Sci., Part A: Polym. Chem.* **2012**, 50, 35-46.

49 B. Mendrek, B. Trzebicka, *Eur. Polym. J.* **2009**, 45, 1979-1993.

50 C. Boyer, A. Atme, C. Waldron, A. Anastasaki, P. Wilson, P. B. Zetterlund, D. M. Haddleton, M. R. Whittaker, *Polym. Chem.* **2013**, 4, 106-112.

51 C. Waldron, A. Anastasaki, R. McHale, P. Wilson, Z. Li, T. Smith, D. M. Haddleton, *Polym. Chem.* **2014**, 5, 892-898.

52 S. R. Samanta, V. Percec, *Polym. Chem.* **2014**, 5, 169-174.

53 N. H. Nguyen, B. M. Rosen, G. Lligadas, V. Percec, *Macromolecules* **2009**, 42, 2379-2386.

54 Q. G. Ma, K. L. Wooley, *J. Polym. Sci., Part A: Polym. Chem.* **2000**, 38, 4805-4820.